Four-dimensional variational assimilation of ozone profiles from the Microwave Limb Sounder on the Aura satellite

Article

Published Version

Four-dimensional variational assimilation of ozone profiles from the Microwave Limb Sounder on the Aura satellite

Liang Feng,[1] R. Brugge,[2] E. V. Hólm,[3] R. S. Harwood,[1] A. O'Neill,[2] M. J. Filipiak,[1] L. Froidevaux,[4] and N. Livesey[4]

Received 3 July 2007; revised 21 December 2007; accepted 7 January 2008; published 25 April 2008.

[1] Ozone profiles from the Microwave Limb Sounder (MLS) onboard the Aura satellite of the NASA's Earth Observing System (EOS) were experimentally added to the European Centre for Medium-range Weather Forecasts (ECMWF) four-dimensional variational (4D-var) data assimilation system of version CY30R1, in which total ozone columns from Scanning Imaging Absorption Spectrometer for Atmospheric CHartographY (SCIAMACHY) onboard the Envisat satellite and partial profiles from the Solar Backscatter Ultraviolet (SBUV/2) instrument onboard the NOAA-16 satellite have been operationally assimilated. As shown by results for the autumn of 2005, additional constraints from MLS data significantly improved the agreement of the analyzed ozone fields with independent observations throughout most of the stratosphere, owing to the daily near-global coverage and good vertical resolution of MLS observations. The largest impacts were seen in the middle and lower stratosphere, where model deficiencies could not be effectively corrected by the operational observations without the additional information on the ozone vertical distribution provided by MLS. Even in the upper stratosphere, where ozone concentrations are mainly determined by rapid chemical processes, dense and vertically resolved MLS data helped reduce the biases related to model deficiencies. These improvements resulted in a more realistic and consistent description of spatial and temporal variations in stratospheric ozone, as demonstrated by cases in the dynamically and chemically active regions. However, combined assimilation of the often discrepant ozone observations might lead to underestimation of tropospheric ozone. In addition, model deficiencies induced large biases in the upper stratosphere in the medium-range (5-day) ozone forecasts.

Citation: Feng, L., R. Brugge, E. V. Hólm, R. S. Harwood, A. O'Neill, M. J. Filipiak, L. Froidevaux, and N. Livesey (2008), Four-dimensional variational assimilation of ozone profiles from the Microwave Limb Sounder on the Aura satellite, *J. Geophys. Res.*, *113*, D15S07, doi:10.1029/2007JD009121.

1. Introduction

[2] Stratospheric ozone plays an important role in atmospheric radiation balance through the absorption of solar and long-wave radiation, while its distribution is controlled by complicated interactions involving atmospheric transport, chemistry and radiation processes. The study of stratospheric ozone has attracted wide scientific and public interest, and many satellite-borne instruments have been developed to provide global ozone monitoring: two recent examples are the Scanning Imaging Absorption Spectrometer for Atmospheric CHartographY (SCIAMACHY) on the Envisat satellite launched in 2002 [*Eskes et al.*, 2005] and the Microwave Limb Sounder (MLS) on the Earth Observing System (EOS) Aura satellite launched in 2004 [*Waters et al.*, 2006].

[3] Efforts have been made to construct three dimensional ozone distributions from space-based observations using various mapping techniques [e.g., *Randall et al.*, 2005], and data assimilation proves to be a powerful tool for this purpose by combining observations with forecasts based on numerical simulation of tracer transport and photochemical processes. In recent years, ozone observations have been assimilated into various chemical transport models (CTMs) driven by off-line winds to generate continuous global ozone fields [*Levelt et al.*, 1998; *Stajner et al.*, 2001; *Errera and Fonteyn*, 2001; *Eskes et al.*, 2003]. In addition, many weather centers have also implemented ozone assimilation into their NWP models [e.g., *Jackson and Saunders*, 2002;

[1]Institute of Atmospheric and Environmental Science, University of Edinburgh, Edinburgh, UK.
[2]Data Assimilation Research Centre, University of Reading, Reading, UK.
[3]European Centre for Medium-range Weather Forecasts, Reading, UK.
[4]Jet Propulsion Laboratory, California Institute of Technology, Pasadena, California, USA.

0148-0227/08/2007JD009121

Struthers et al., 2002; *Geer et al.*, 2006; *Jackson*, 2007]. At the European Centre for Medium-range Weather Forecasts (ECMWF), assimilation of ozone layer observations from the Solar Backscatter Ultraviolet instruments (SBUV on NIMBUS-7 and SBUV/2 on several NOAA satellites) and total ozone columns from other nadir instruments were first implemented into the ECMWF 45-year reanalysis project ERA-40 before becoming operational in 2002 [*Dethof and Hólm*, 2004].

[4] In these weather centers, ozone assimilation is mainly motivated by its potential beneficial impacts on meteorological fields, one of which is to improve the use of satellite radiance by providing observation operators with realistic 3D ozone fields instead of the climatology. With advances in remote sensing technology, the vertical resolution of space-based instruments has been significantly improved in the recent years. In principle, a full use of radiance information from instruments of high vertical resolution requires a detailed, highly accurate, description of the vertical of distribution of ozone. However, owing to limited computational resources, ozone chemical schemes implemented in NWP models are usually very simple, and have some known difficulties [e.g., *McCormack et al.*, 2006; *Geer et al.*, 2007]. On the other hand, owing to the coarse vertical resolution of the operational ozone observations in the lower stratosphere, the vertical structure of the analysis increments in the operational ECMWF data assimilation system is mainly determined by the background error covariances [see, e.g., *Dethof and Hólm*, 2004]. As a result, operational ozone analyses usually show large errors in the lower stratosphere where radiation absorption by ozone is an important component of the atmospheric energy budget. Moreover, when a 4D-var data assimilation scheme is employed, ozone assimilation could provide constraints on stratospheric wind fields, which are poorly observed directly. But the inconsistencies in the analyzed ozone fields mean that such impacts are not always beneficial [*Riishøjgaard*, 1996; *Hólm et al.*, 1999, 2000; *Peuch et al.*, 2000].

[5] We seek to improve ozone analyses in the ECMWF data assimilation system by including ozone profiles from the Microwave Limb Sounder on the EOS Aura satellite. Aura MLS is an advanced version of the MLS experiment on the Upper Atmosphere Research Satellite (UARS), providing near-global continuous measurements of ozone between 215 and 0.46 hPa (for the version 1.5 retrievals) with a typical vertical resolution of 2.7 km in the middle stratosphere.

[6] This work is directly inspired by the experiment by *Dethof* [2003] for assimilating ozone profiles from the Michelson Interferometer of the Passive Atmospheric Sounding (MIPAS) into the ECMWF weather forecasting system. Her results showed that assimilating the detailed vertical structure of the MIPAS ozone profiles can substantially improve ozone analyses in the tropical lower stratosphere where the model tended to underestimate the ozone peak value, and also inside the winter vortex, where ozone transport and chemical depletion were difficult to model accurately. Similar results were obtained in other recent experiments for assimilating profiles from passive limb sounding instruments, like UARS MLS and MIPAS, into different GCM or CTM models [e.g., *Struthers et al.*, 2002; *Wargan et al.*, 2005; *Geer et al.*, 2006]. For example, beneficial impacts were found from the assimilation of solar occultations, although such observations were sparse and had very limited latitude coverage [*Stajner and Wargan*, 2004; *Stajner et al.*, 2006].

[7] Compared with the observations used in the previous experiments, Aura MLS has a wider and much denser spatial coverage, while showing good quality in a broad vertical range. In addition, this instrument has been working in a stable state since it was launched in 2004. So, assimilation of MLS ozone profiles is expected to generate reliable and consistent stratospheric ozone fields for scientific research and model evaluation.

[8] Like other weather centers [see, e.g., *Jackson*, 2007], ECMWF and the Data Assimilation Research Centre (DARC), UK, have made several experiments for assimilating MLS observations since 2005. The present paper is focused on one long experiment for a 95-day period from 13 August to 15 December 2005 to evaluate the impacts of the extra constraints provided by MLS ozone data on ozone analyses. Such a long experiment is of both scientific and practical interest, as it is planned to assimilate the near-real-time (NRT) MLS ozone retrievals operationally in the near future.

[9] The next section gives a simple description of the ozone assimilation system, the assimilated ozone observations, as well as the independent observations used to evaluate the resulting ozone analyses. In the third section, the impacts from assimilating MLS ozone profiles are evaluated by comparing the control (without MLS ozone profiles assimilated) and assimilation run with independent observations in several latitude bins. Our results show that MLS data substantially improve the agreement of the analyzed ozone fields with independent observations. In particular, as indicated by case studies, the resulting ozone analyses well capture the spatial and temporal variations related to both chemistry and dynamics. Finally, conclusions are presented in the fourth section.

2. Ozone Observation and Assimilation System

2.1. Assimilation System

[10] The present experiment is based on version CY30R1 of the operational ECMWF data assimilation system (the reader is referred to http://www.ecmwf.int/research/ifsdocs for a detailed description on ECMWF data assimilation systems). In the ECMWF system [*Dethof and Hólm*, 2004], ozone mass mixing ratio is fully integrated as an additional variable governed both by tracer transport and by chemistry production/loss. The latter processes are modeled by a relaxation toward chemical equilibrium. Specifically, the net chemical generation rate ($P - L$) at a model grid point is given by the first-order Taylor expansion around the chemical equilibrium [*Cariolle and Déqué*, 1986],

$$\frac{dO_3}{dt} = P - L = \overline{P-L} + C_1\left(O_3 - \overline{O}_3\right) + C_2\left(T - \overline{T}\right) + C_3\left(A - \overline{A}\right) + C_4 O_3, \quad (1)$$

where O_3 is the ozone mass mixing ratio at the given grid point, T the temperature, and A the column of ozone overlying the grid level. In the above equation, $\overline{P-L}$ and the corresponding reference states, such as the ozone mixing

ratio $\overline{O_3}$, mean temperature $\overline{T}$, and the overlying ozone column $\overline{A}$, are all functions of the latitude, pressure and month, and were determined from a 2D photochemical model containing a representation of the heterogeneous ozone hole chemistry [*Cariolle and Teyssédre*, 2007]. The coefficients C_i, $i = 1, 2, 3$ were also derived from the same 2D model by perturbation, while the fifth term in equation (1) is used to model the heterogeneous sinks, and is only turned on in sunlight when the temperature is below 195 K.

[11] The early version (Cariolle v1.0) of the adopted ozone photochemistry parameterization was found to have some deficiencies, such as the unrealistically strong impacts from the overlying ozone column on the net ozone generation rate [*McCormack et al.*, 2006; *Geer et al.*, 2007]. So, a recently revised scheme Cariolle v2.3 is implemented into CY30R1. Note that we use ozone climatology [*Paul et al.*, 1998] instead of the fields from the 2D photochemical model as the reference ozone distribution $\overline{O_3}$ and $\overline{A}$, since the ozone climatology is expected to be less biased with respect to observations [*Eskes et al.*, 2003; *Dethof and Hólm*, 2004].

[12] As mentioned before, for comparison, one assimilation run (referred to as MLSA hereafter) and one control run (referred to as CTRL hereafter) have been completed for the autumn of 2005 to track the ozone variation associated with formation and breakdown of polar vortices in the northern and southern hemisphere, respectively. The control run assimilates the operational ozone observations from SBUV/2 and SCIAMACHY, whereas the assimilation run includes the MLS ozone profiles as additional constraints. Except for the different usage of MLS data, the assimilation and control runs share the same model configuration. Both of them use the same 4D-variational data assimilation scheme with 12-hour data assimilation window, and are run at a horizontal resolution T159 (i.e., about 1.125° in the latitude and longitude directions), with 60 vertical levels from the Earth surface to 0.1 hPa. They also assimilate the same comprehensive set of operational observations of meteorological fields, which include radiance from nadir instruments such as AMSU (Advanced Microwave Sounding Unit) and AIRS (Atmospheric InfraRed Sounder). Note that both the control and assimilation runs adopt the same initial ozone background error covariances with a structure similar to that described by *Dethof and Hólm* [2004].

[13] Ozone observations affect the forecast of other variables only through changing the initial state, since the present experiments use the ozone climatology in the radiation calculation, rather than the model ozone itself. This is motivated by the fact that interactive ozone in radiation has so far not proved beneficial, and hence has not been adopted by the operational ECMWF weather forecasts [*Morcrette*, 2003]. The changes to the meteorological fields from ozone observations come both from the use of the model ozone fields in the assimilation of radiance observations and through the coupling of trace gas concentrations and air transport. The feedbacks to meteorological fields are usually small, with the effect of MLS (differences between the assimilation and control runs) on the zonal mean temperature differences generally smaller than 0.2 K at levels below 10 hPa, increasing to about 1.0 K at the top of the model. Preliminary results also reveal some noticeable changes in the wind fields, in particular, in the tropical upper stratosphere. But the interpretation and quantification of these impacts require further investigations, and will be detailed in other places.

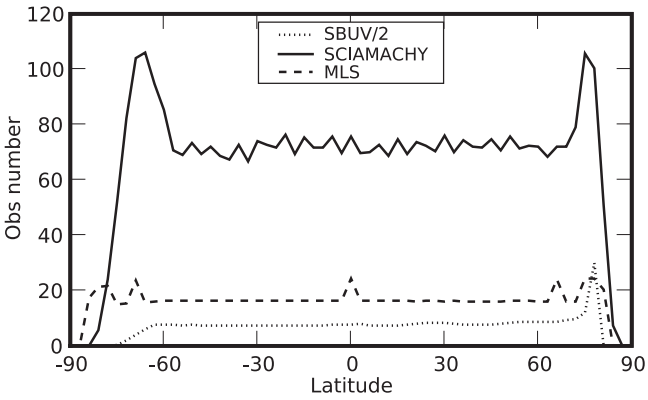

Figure 1. The daily number of the assimilated ozone profiles per 1° latitude from SCIAMACHY (solid line), MLS (dashed line), and SBUV/2 (dotted line), averaged for September 2005.

2.2. Assimilated Ozone Observations

[14] SCIAMACHY is an ultraviolet (UV)/Visible/near-infrared (NIR) spectrometer onboard Envisat, which was launched in 2002. The SCIAMACHY total ozone column is retrieved from measurements of backscattered ultraviolet and visible solar radiation using the TOSOMI algorithm [*Eskes et al.*, 2005]. SCIAMACHY has a high-density horizontal coverage (see Figure 1). Daily, about 12,000 SCIAMACHY observations are assimilated into our experiments. During September the sunlit region observed by SCIAMACHY extends southward from 70°S on 1 September to around 80°S on 30 September. Thus the degree to which the polar vortex is sampled changes markedly at a time when strong ozone depletion occurs. Comparisons with the Global Ozone Monitoring Experiment (GOME) as well as some ground-based observations suggest that SCIAMACHY underestimates total ozone columns by 1.5–1.7% [*Eskes et al.*, 2005]. For more details on SCIAMACHY, the reader is referred to www.sciamachy.org.

[15] The SBUV/2 instrument is a scanning double monochromator, measuring backscattered solar radiation in 12 discrete wavelength bands from 252.0 to 339.8 nanometers. In our experiment, the version 8 retrievals from the SBUV/2 on the NOAA-16 satellite are assimilated (see http://avdc.gsfc.nasa.gov/Data/Browse/sbuv2.html for details). Owing to its nadir viewing geometry and limited frequency range, SBUV/2 has a coarse vertical resolution [*Bhartia et al.*, 1996]. Hence, the retrieved ozone given for 12 layers are converted to partial ozone columns for six layers: 0.1–1 hPa, 1–2 hPa, 2–4 hPa, 4–8 hPa, 8–16 hPa, and 16 hPa to surface, to avoid vertical error correlations, which have not been modeled in our assimilation. Note that the lowest layer is chosen to be rather thick (16 hPa to surface), because SBUV/2 is insensitive to the vertical distribution of ozone below the ozone maximum in the stratosphere [*Fioletov et al.*, 2006; *Wargan et al.*, 2005]. Another drawback of the SBUV-like instruments is that they only measure in daylight, and for quality control, the observa-

tions with solar zenith angle larger than 84° are rejected. As a result, the assimilated SBUV/2 observations cover only north of 62°S on September 1, before reaching 74°S on September 30. Daily, about 1200 SBUV/2 profiles are assimilated into both the assimilation and control runs (Figure 1).

[16] MLS on the Aura satellite is designed to provide near-global continuous measurements of temperature, and geopotential height as well as a rich set of chemically important trace constituents such as H_2O, O_3, N_2O, HNO_3, and ClO in the stratosphere and upper troposphere. Thermal emissions from the upper tropospheric and stratospheric ozone are observed by four different MLS radiometers designated R2, R3, R4, and R5 at frequencies near 190 GHz, 240 GHz, 640 GHz and 2.5 THz, respectively. But, the MLS ozone profiles assimilated in our experiment are the standard products of version 1.51, which are retrieved using only radiometer R3 (together with the temperature measurement from radiometer R1A/B near 118 GHz). The version 1.51 ozone profiles are retrieved as piecewise linear in log pressure, with 6 regularly spaced node points per factor ten in pressure (i.e., 316, 215, 147, 100, 68.1, 46.4 hPa, and so on), giving an effective vertical resolution of about 2.7 km [*Froidevaux et al.*, 2006]. Note that although MLS observations contain useful information on ozone concentrations between 316 hPa and 0.1 hPa, only the data between 215 and 0.46 hPa are recommended for scientific research. Compared to other limb sounders such as MIPAS and UARS MLS, Aura MLS provides more dense horizontal coverage; as shown in Figure 1, its daily 3500 profiles are quite evenly spread between 82°S and 82°N, while MIPAS can only produce up to 1000 profiles every day, and UARS MLS about 1300 profiles. Also, the two-dimensional retrieval algorithm has improved the horizontal resolution along the line of sight to about 200 km.

[17] In general, MLS ozone profiles are in good agreement with SAGE II (Stratospheric Aerosol and Gas Experiment) and HALOE (Halogen Occultation Experiment) observations, with its bias from HALOE measurements between 100 hPa and 1 hPa being less than 5% [*Froidevaux et al.*, 2006]. It is also found that version 1.51 has slightly more ozone in the lower stratosphere (by a few percent) and less ozone in the upper stratosphere (by up to 10% at 1 hPa), when compared to the new (version 2.2) MLS data set [*Froidevaux et al.*, 2008]. Moreover, a recent study by *Yang et al.* [2007] shows that the stratospheric ozone columns of the version 1.51 data set are higher than SAGE II observations by about 3 Dobson units (DU). In the experiment, we only use version 1.51 data flagged as good. Also, considering the possible vertical and horizontal correlations in the retrieved profiles, we enlarge the errors associated with the retrieved ozone mixing ratios by 50% of the officially estimated errors given as part of the standard products.

[18] Like other experiments for assimilation of ozone observations [*Struthers et al.*, 2002; *Dethof*, 2003; *Jackson*, 2007], we do not attempt to remove possible biases from ozone observations before assimilation, mainly because of the difficulty in knowing the 'truth'. As a result, there may be systematic differences existing between different observations. Here, as an example, some systematic differences between the operational observations and MLS ozone data are presented in Figure 2 for the monthly means of ozone

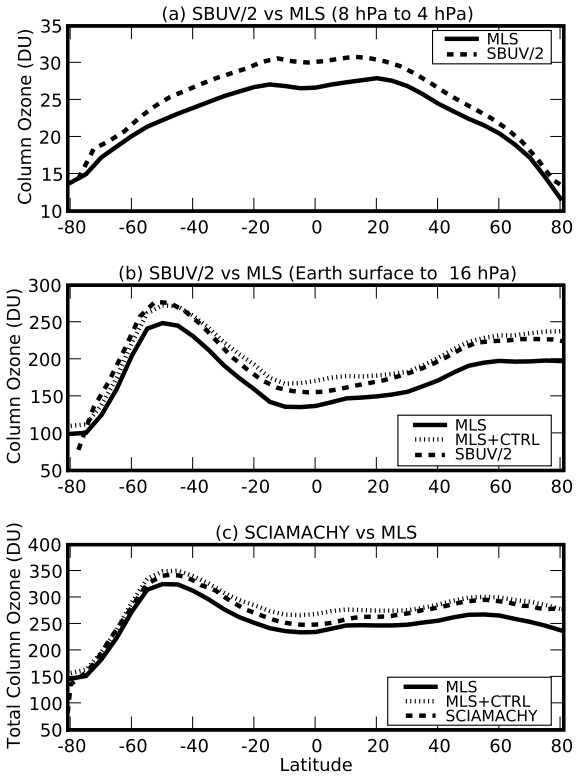

Figure 2. (a) The zonally averaged MLS (solid line) and SBUV/2 (dashed line) partial ozone columns (in Dobson unit, (DU)) at the 4–8 hPa layer during September 2005. (b) Comparison of the zonally averaged SBUV/2 partial ozone column (dashed line) at the 16 hPa to surface layer against the sum (dotted line) of the zonal mean ozone column of MLS data between 215 and 16 hPa, and the zonal mean ozone column of the control run between the Earth surface and 215 hPa. Note that the solid line represents the partial ozone column between 215 and 16 hPa derived from MLS observations. (c) The same as Figure 2b but for the comparison between SCIAMACHY total ozone columns and the ones derived from MLS observations between 215 hPa and 0.46 hPa and the ozone analyses between the Earth surface and 215 hPa in the control run.

columns. In the upper stratosphere between 4 and 8 hPa (Figure 2a), SBUV/2 shows systematically more ozone than MLS data at almost all latitudes, with largest departures seen between 20°S and 20°N. We note that upper stratospheric ozone abundances from the new (version 2.2) MLS data set are a few percent larger than the version 1.51 values [see *Froidevaux et al.*, 2008], which reduces but does not eliminate the discrepancy versus SBUV/2 in this region. In fact, as revealed by the comparisons with SAGE II observations [*Nazaryan and McCormick*, 2005], the SBUV/2 data set from the NOAA-16 satellite shows a systematic overestimation of the upper stratospheric ozone.

[19] In contrast, in the lower stratosphere, SBUV/2 on NOAA-16 usually tends to underestimate ozone concentrations [*Terao and Logan*, 2007], while MLS version 1.51

have small positive biases [*Yang et al.*, 2007; *Froidevaux et al.*, 2008]. Since the SBUV/2 observations between 16 hPa and the surface layer are assimilated as a single partial ozone column, the systematic differences between SBUV/2 and MLS observations in the lower stratosphere can eventually lead to substantial underestimation of the tropospheric ozone, when they are assimilated together. This is schematically demonstrated in Figure 2b where the monthly mean of SBUV/2 ozone column at the 16 hPa to surface layer is compared with the sum of the zonal mean ozone column of MLS observations between 16 and 215 hPa and the zonal mean ozone column of the control run between the Earth surface and 215 hPa. Clearly, when MLS data between 16 and 215 hPa are added to the data assimilation system, the ozone at the lower lying levels will have to be significantly reduced to reproduce the ozone columns from SBUV/2. Moreover, Figure 2b indicates that the underestimation by SBUV/2 at 30°S–80°N amounts to 5–40% of the ozone content between the Earth surface and 215 hPa, although these amounts are small compared to the whole ozone column from the Earth surface to 16 hPa. As a result, the underestimation of the tropospheric ozone is well observed in the comparisons of the assimilation run with ozone sondes presented later, despite the usual overestimation of the tropical tropospheric ozone by the ECMWF operational data assimilation systems [*Dethof and Hólm*, 2004]. It is also noted (Figure 2c) that the total ozone columns from SCIAMACHY are also considerably lower than that suggested by the MLS (and the control run) in the low latitudes, owing to the overestimation of stratospheric ozone columns by MLS version 1.51 data, and the underestimations of the total columns by SCIAMACHY [*Eskes et al.*, 2005] (as well as the overestimation of the tropical tropospheric ozone from the Earth surface to 16 hPa by the control run). Such biases can also play a part in degrading tropospheric ozone analyses around the tropics, as an adverse effect of the joint assimilation of MLS and operational ozone observations.

2.3. Independent Ozone Observations for Evaluation

[20] In the present paper, ozone observations from the Polar Ozone and Aerosol Measurement (POAM III), SAGE III, ozone sonde, and ground-based microwave radiometers are used to evaluate the analyzed ozone fields in the control and assimilation runs.

[21] POAM III is a solar occultation instrument, providing measurements of ozone, NO_2, H_2O and aerosol extinction with vertical resolution of about 1 km. Daily, POAM III makes 14–15 sunset and sunrise measurements along two latitude circles in the southern and northern hemispheres, respectively. In each year, the northern circle changes between 54°N and 71°N, and the southern between 63°S and 68°S. *Randall et al.* [2003] have compared POAM III with other satellite and ozone sonde data, and found that the agreement is within 5% between 13 and 60 km. In our comparison, the data of version 4.3 are used.

[22] SAGE III measures trace gases and aerosols by measuring the solar and lunar occultation in the frequency range from 289 nm to 15145 nm [*Thomason and Taha*, 2003]. The retrieved ozone profile has a vertical resolution of about 1 km, and its random error is reported not to exceed 3% between 50 and 8 hPa [*Thomason and Taha*, 2003]. The version 4 data are used in our comparison. Owing to the limited availability of the lunar occultations during the experiment period, we only use SAGE III solar occultations, which have a limited latitude coverage, and provide observations only on the middle latitudes in the southern hemisphere, and the high latitudes in the northern hemisphere.

[23] Ozone sonde data were obtained from the World Ozone and Ultraviolet Radiation Data Centre (WOUDC) (www.woudc.org), and the Southern Hemisphere Additional Ozonesondes (SHADOZ) network [*Thompson et al.*, 2003]. The ozone data from 36 stations were used in our comparison, and most of them are obtained by Electrochemical Concentration Cell (ECC) sensors. The typical error of ECC sondes is within −7% to 17% in the middle and upper troposphere, and ±15% in the lower stratosphere [*Komhyr et al.*, 1995]. When ozone amounts are very low, their uncertainty could be higher. In addition, measurements by the ground-based microwave radiometers at 4 sites, i.e., Bern (Switzerland), Payerne (Switzerland), Mauna Loa (Hawaii), and Lauder (New Zealand) from the Network for the Detection of Atmospheric Composition Change (NDACC), have also been used in the present validation because of their ability to detect ozone in the upper stratosphere (See http://www.iapmw.unibe.ch/research/collaboration/ndsc-microwave for details).

3. Impacts of Assimilating MLS Ozone Profiles

3.1. Overview

[24] Figure 3a shows the pressure-latitude cross section of the zonal mean differences between MLS observations and the ozone analyses before MLS ozone profiles are assimilated. The results have been averaged for the whole experimental period from mid-August to mid-November 2005, and essentially pick up the areas with large systematic deficiencies in the operational ozone assimilation, considering the good agreement of MLS data with independent observations such as HALOE and SAGE II.

[25] During the experiment period, stratospheric ozone inside the winter vortex around the southern high latitudes experienced rapid heterogeneous depletion following the arrival of sunlight. The data assimilation systems containing Cariolle v1.0 photochemistry parameterization scheme usually cannot well reproduce such rapid ozone depletion, leading to overestimation of ozone values inside the winter vortex [*Dethof*, 2003]. However, with the implementation of Cariolle v2.3, the model now tends to show larger vertical range of severe ozone depletion inside the winter vortex than that suggested by MLS observations, evidenced by the underestimation of ozone around 20 hPa south of 70°S by up to 0.5 ppmv (Figure 3a). Similar underestimation is also apparent in the comparisons of the control run with POAM III and ozone sondes at the southern high latitudes (see section 3.2). Moreover, as shown in Figure 4, the 5-day forecasts based on the assimilation run show a similar pattern of overestimated ozone loss inside the winter vortex in the five days following the assimilation, suggesting that the underestimation of ozone around 20 hPa is directly attributable to the ozone chemistry described by the data assimilation system. Because the operational ozone observations only provide limited coverage of the southern high

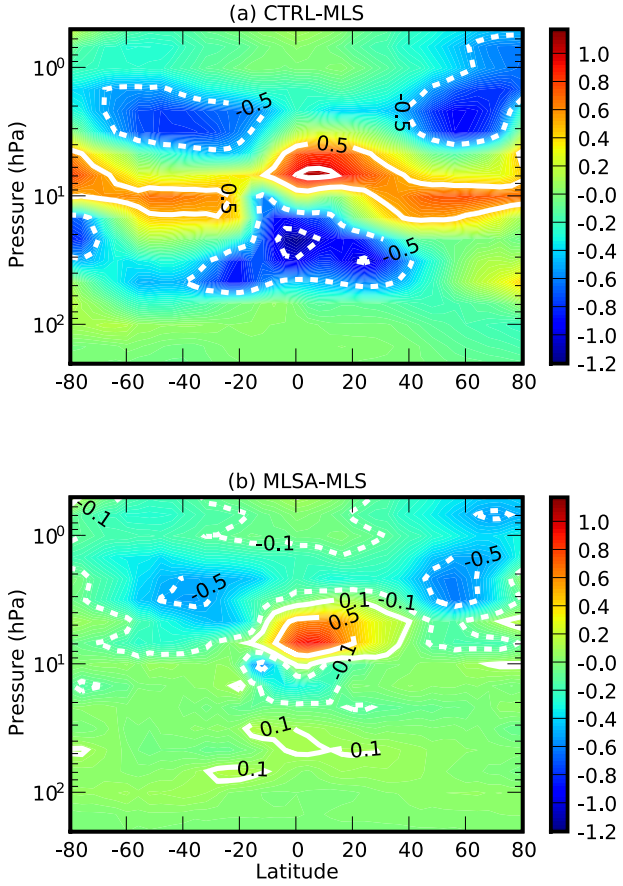

Figure 3. Biases in the ozone analyses (in ppmv) in (a) the control run and (b) the assimilation run with respect to MLS observations during the 95-day experiment period.

latitudes, without any information on the vertical structure in the middle and lower stratosphere, the analysis increments from assimilating SCIAMACHY and SBUV/2 observations are spread to different levels at the vortex core purely through the background error covariance, resulting in little correction of the low model ozone values around 20 hPa, south of 70°S (Figure 3a). In contrast, when MLS profiles are assimilated, such underestimation is effectively corrected (Figure 3b).

[26] Another well documented problem for the systems assimilating only SBUV-like observations is the underestimation of the peak value of the ozone partial pressures in the tropical lower stratosphere, which is thought to be associated with model deficiencies in tracer transport [see, e.g., *Wargan et al.*, 2005; *Schoeberl et al.*, 2003]. In the lower stratosphere, ozone is long-lived, meaning that significant biases in the transport could have substantial impacts on ozone forecast and analyses. *Geer et al.* [2006] showed that extremely fast upwelling in their data assimilation system tended to reduce the value of the ozone peak. Similar underestimation is observed in our control run between 10 and 50 hPa (Figure 3a), and is again well corrected by assimilating MLS data (Figure 3b).

[27] Between 5 and 10 hPa, when compared to MLS observations, the control run overestimates ozone mixing ratios at nearly all latitudes, with largest overestimation of about 1.0 ppmv just over the equator. In principle, the exaggerated upwelling over the tropical regions may carry extra ozone into the higher vertical levels, resulting in overestimation of the ozone distributed above the ozone peak. But the widely spread overestimation in the control run is more likely to be caused by the positive biases in SBUV/2 observations, and by the possible small negative biases in MLS (Figure 2a). On the other hand, the 5-day ozone forecasts (see Figure 4) show similar vertical range of overestimation, but of a much smaller magnitude.

[28] It is also noted that even after assimilation of MLS ozone profiles, the resulting ozone fields are still considerably larger (up to 0.5 ppmv) than MLS observations between 5 and 10 hPa at the low latitudes (Figure 3b), in contrast to the effective correction of the overestimation at all other latitudes. We found that the persistent overestimation in the tropical middle stratosphere is related to the high rejection rate for MLS observations between 5 and 10 hPa at the low latitudes (Figures 5a and 5b). Moreover, as shown in Figure 5c, the rejection of MLS observations between 4.6 and 6.8 hPa by quality control processes embedded in the variational data assimilation is a direct result of large departures of the observations from the short-term (0–12 hours) model forecasts made from the analyses contaminated with significant overestimation of ozone in the tropical middle stratosphere. In addition, high rejection rates are also found at the 6.8–10 hPa layer (not shown here) over the tropic regions.

[29] At the higher levels (1–5 hPa), the control run tends to underestimate the ozone values (Figure 3a). Such underestimation can be attributed to the model bias, as the ozone analyses have considerably lower zonal mean values than SBUV/2 observations, although they have been assimilated into the control run. In particular, Figure 4 suggests that the model underestimation develops quickly, reaching beyond −0.5 ppmv at the middle latitudes in the 5-day forecasts. Interestingly, *McCormack et al.* [2006] noted similar underestimation equatorward of 30°N in their simulations based on a CTM embedded with the ozone photochemistry parameterization Cariolle v2.1. This underestimation is thought to be caused by the systematic temperature differences between their CTM model and the reference temperature $\overline{T}$ [*McCormack et al.*, 2006; *Geer et al.*, 2007]. Further

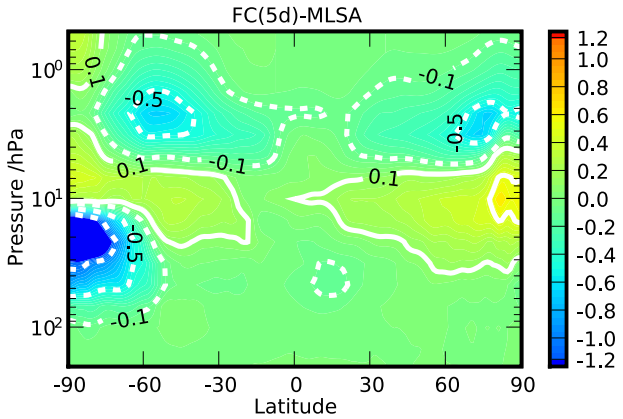

Figure 4. The zonal mean of the errors (in ppmv) in the 5-day ozone forecasts of the assimilation run with respect to the corresponding analyses. The results are averaged over 16 forecasts starting at 1200 UT, 5–20 September.

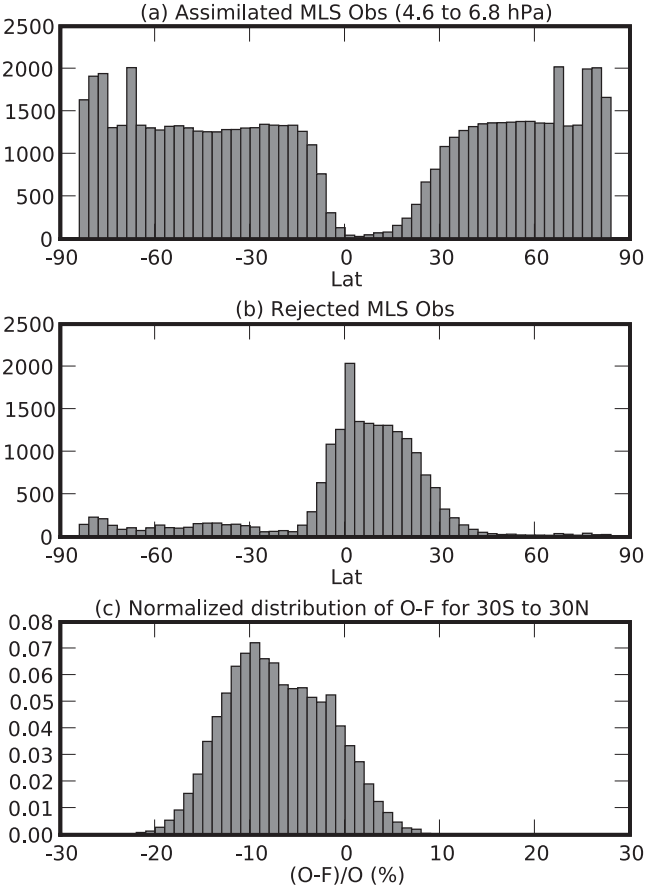

Figure 5. (a) The total number of the assimilated MLS observations at the 4.6–6.8 hPa layer per 3° latitude during October 2005. (b) The same as Figure 5a but for the rejected observations. (c) The normalized distribution of the departures of MLS observations from the 6-hour forecasts (O-F) at the 4.6–6.8 hPa layer in the assimilation run during October 2005.

examination reveals the similar cause for the underestimation shown in Figure 3a: the systemically warmer upper stratospheric temperature of the data assimilation system drives the zonal mean ozone to be less than the ozone climatology. Moreover, owing to the short ozone photochemical relaxation time in the upper stratosphere (except in the polar night) [*McCormack et al.*, 2006], the coarse spatial and temporal coverage of SBUV/2 data failed to correct these negative model biases, and even the improvements shown in Figure 3b from assimilation of more dense MLS data are not fully reproduced in the comparisons with independent observations (see next subsection).

[30] In the middle stratosphere, local ozone production rates are sensitive to the amount of ozone in the overlying layers owing to their absorption of the incident solar radiation. Such effects are described by the fourth term in equation (1) while being represented in the background error covariance as anticorrelations between the lower and upper layers in the middle and upper stratosphere. As a result, assimilation of MLS profiles at 1–10 hPa not only corrects the overestimation of ozone around 7 hPa, but eventually drives the analyses at latitudes 30°S–60°S to a value slightly lower than MLS observations, owing to the negative correction induced by the analysis increment at higher altitudes (Figure 3b).

3.2. Comparison With Independent Ozone Observations

[31] The ozone analyses in the control and the assimilation run are evaluated through comparisons with independent observations in different latitude bins. In these comparisons, ozone analyses are temporally and spatially interpolated to the time and horizontal location of the observations. Necessary vertical interpolation (or smoothing for ozone sondes) has also been applied to project both the observed and analyzed ozone profiles to the standard MLS pressure grid so that appropriate statistics could be made.

3.2.1. Northern High Latitudes: 60°N–90°N

[32] In Figure 6, ozone analyses from the assimilation and control run are compared with SAGE III and POAM III observations. The comparisons exhibit substantial improve-

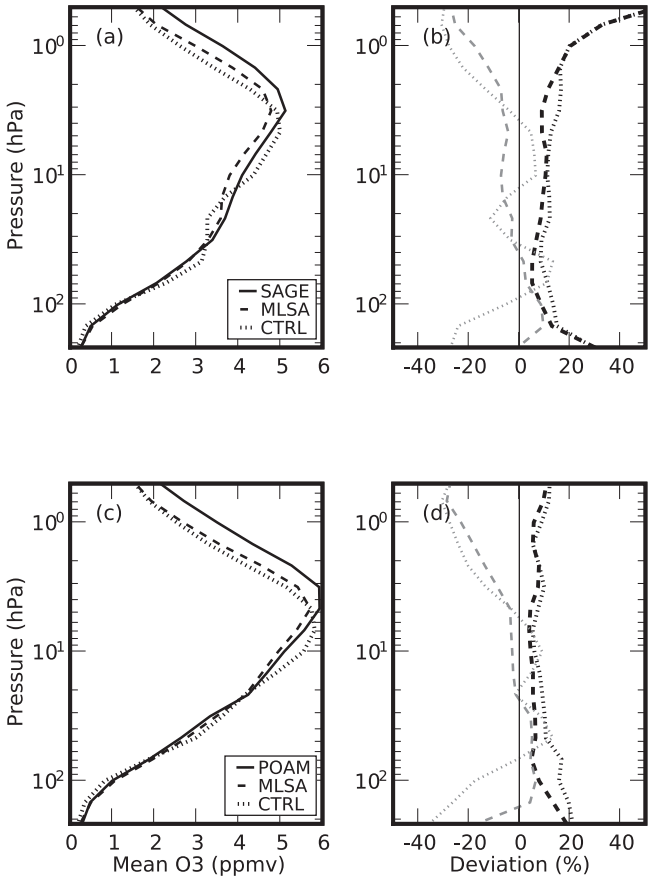

Figure 6. (a) The mean ozone profile from SAGE III observations (solid line) at the northern high latitudes is compared with the collocated analyses in the assimilation run (dashed line) and the control run (dotted line) during 13 August to 15 November 2005. (b) The mean bias (grey dashed line) and the standard deviation (dark dashed line) of the assimilation run with respect to SAGE III observations at the northern high latitudes (in the percentage of the mean observation values) are compared with the results for the control run shown as the dotted lines. (c) and (d) The same as Figures 6a and 6b, respectively, but for the comparisons with POAM III.

ments in the analyses at the northern high latitudes covered by SAGE III when MLS data are assimilated (see Figures 6a and 6b). MLS data reduce the mean ozone mixing ratio by up to 0.5 ppmv at both the middle stratosphere between 5 and 20 hPa, and the lower stratosphere between 100 and 40 hPa, resulting in a better agreement with SAGE III mean profile between 100 and 40 hPa, and a slight underestimation between 5 and 10 hPa. The positive increment of 0.3 ppmv around 20 hPa also contributes to the improved agreement with SAGE III. Following the inclusion of MLS ozone data, there is a significant decrease in the standard deviation between 150 and 1.5 hPa. In particular, the standard deviation around 100 hPa has been reduced from 10% to less than 5%, in contrast to other experiments which found little impacts at such low altitudes from assimilating MIPAS ozone profiles [*Dethof*, 2003; *Wargan et al.*, 2005; *Geer et al.*, 2006]. Basically, such improvements reflect the good quality of MLS data at the lower stratosphere around 100 hPa.

[33] During the autumn of 2005, POAM III observed the latitude band 63°N–65°N. Figures 6c and 6d show that the inclusion of MLS data improves the agreement of the analyses with POAM III data, with standard deviation around 100 hPa reduced from about 20% to about 10%. The comparisons with ozone sondes (Figures 7a and 7b) further confirm the substantial improvement in the ozone analyses between 10 and 200 hPa. Note that Figure 7 displays the mean ozone concentrations as partial pressures instead of volume mixing ratios to highlight the ozone vertical distribution in the lower stratosphere and upper troposphere. Clearly, MLS data successfully correct the negative bias between 100 and 200 hPa in the control run, increasing the mean ozone partial pressure by up to 4 mPa, while reducing the standard deviation at 100 hPa from about 12% to 7%.

[34] However, as shown in Figure 7a, although there is no MLS observation for levels below 215 hPa, the improvements in the stratosphere adversely lead to an underestimation of the tropospheric ozone, mainly due to the constraints from the negatively biased SBUV/2 partial ozone columns (Figure 2b).

[35] In addition, in the upper stratosphere, despite the gains from MLS data, the resulting analyses still underestimate the ozone mixing ratios by 10–30% (Figures 6a and 6c). This is related to the short ozone photochemical relaxation time in the upper stratosphere. Also, the version 1.51 MLS ozone profiles possibly have small low biases in this region [*Froidevaux et al.*, 2008].

3.2.2. Middle Latitudes: 30°N–60°N and 30°S–60°S

[36] Figures 7c and 7d compare the ozone analyses in the assimilation run and the control run with ozone sondes at the northern middle latitudes. In general, improvement in the mean profile is modest, when compared with that seen in the high latitudes. But the reduction in the standard deviation between 200 and 10 hPa is still significant: the standard deviation around 100 hPa is reduced from about 25% to about 18%. Another major improvement is the increase of the peak ozone partial pressure by about 1 mPa around 30 hPa, resulting in a better agreement with observations.

[37] In the southern middle latitudes (Figures 7e and 7f), the impact on the mean profile between 10 and 100 hPa is quite small, as the control run is already in good agreement with ozone sondes, which are only available at Lauder station (45°S), New Zealand for the experiment period. Here, the main benefit of MLS data is the reduction of the standard deviation between 10 and 50 hPa from 4–10% to below 5%.

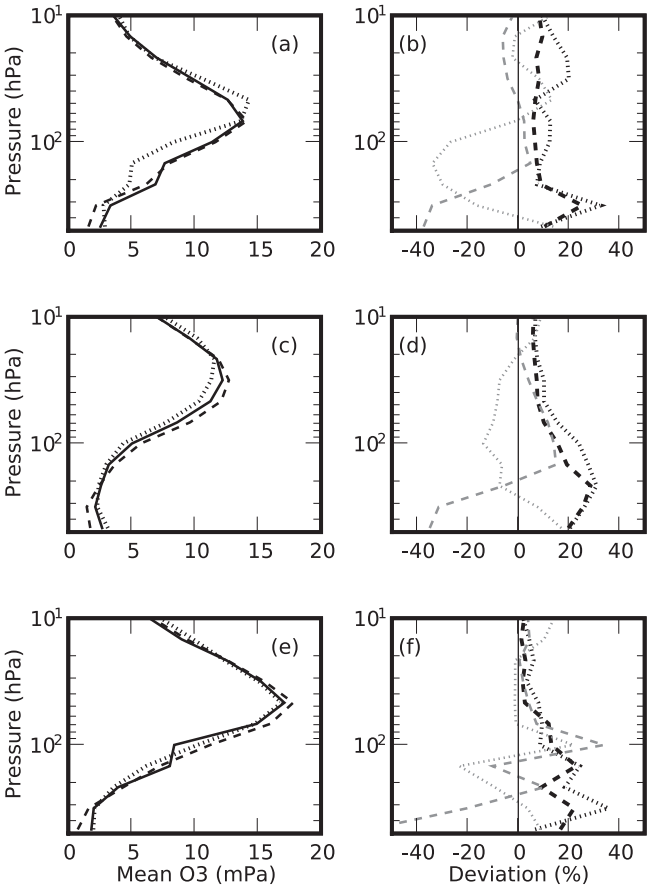

Figure 7. (a and b) Similar to Figures 6a and 6b, respectively, but for the comparisons with ozone sondes at 60°N–90°N. Note that the mean ozone concentrations are given as partial pressures (in mPa) instead of volume mixing ratios to highlight the vertical distribution in the upper troposphere and lower stratosphere. (c and d) The same as Figures 7a and 7b, respectively, but for the comparisons with ozone sondes at the northern middle latitudes (30°N–60°N), and (e and f) the results for the southern middle latitudes.

[38] The comparisons with SAGE III and the ground-based microwave radiometers (Figure 8) further confirm the general improvement in the ozone analyses between 10 and 100 hPa from assimilation of MLS ozone profiles. However, obvious gains from MLS data still could not fully correct the model low biases in the upper stratosphere, as discussed before.

[39] During the experiment period, the northern middle latitudes are under complicated meteorological conditions associated with the formation of the polar vortex during the late northern autumn. As one example, Figures 9a and 9b depict the maps of the potential vorticity, geopotential height, temperature and ozone analyses at 10 hPa over the

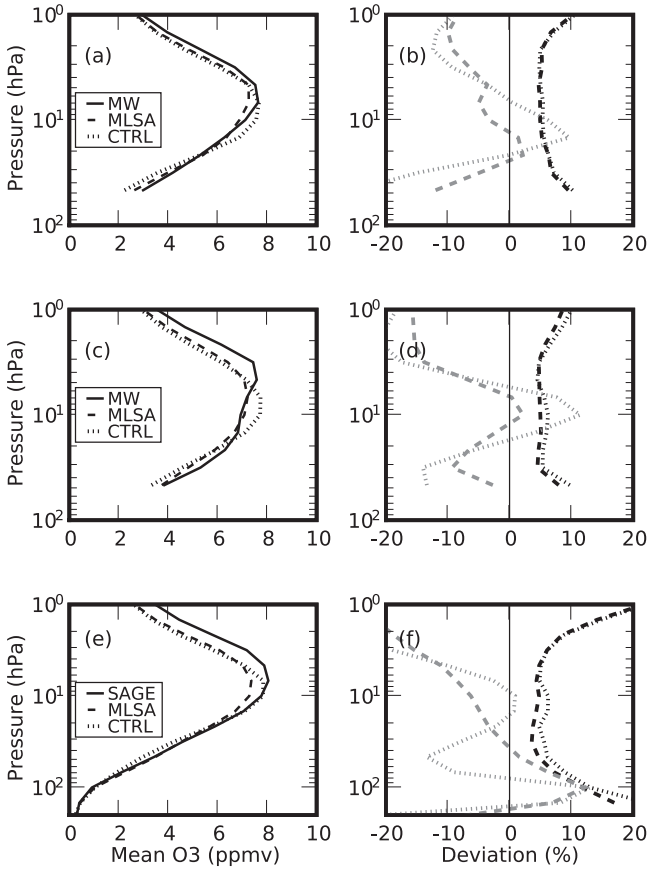

Figure 8. (a and b) The same as Figures 6a and 6b, respectively, but for comparison with ground-based microwave (MW) radiometers at Bern (47.0°N, 7.4°E) and Payerne (46.8°N, 7.0°E). (c and d) The same as Figures 8a and 8b, respectively, but for the station at Lauder (45.0°S, 169.7°E). (e and f) The comparison of ozone analyses with SAGE III observations at the southern middle latitudes.

northern hemisphere on 9 November 2005. The potential vorticity, as well as the temperature and geopotential height, reveals a developing but well-defined polar vortex, with its core displaced from the northern pole to (75°N, 80°E) by one anticyclone around (65°N, 120°E). In addition, the prototype vortex is gradually isolated from the ozone-rich air from low latitudes, showing much lower ozone values than the outside air (Figure 9b).

[40] We now examine the ozone profiles at three sonde sites denoted as the white triangles in Figure 9, which are chosen for their different meteorological conditions: the station at (80°N, 86°W) is located between the vortex and the thin filament of ozone-rich air drawn up from low latitudes; the second one is at (79°N, 12°E) right inside the polar vortex, and the third one is at (52°N, 14°E), falling within the wide tongue of the material drawn off from the vortex edge. However, the polar vortex at the lower altitudes is less developed, evidenced by the much smaller and distorted polar vortex at 32 hPa (Figures 9c and 9d). In particular, the area around (52°N, 14°E) has its ambient air originating in low latitudes.

[41] These meteorological differences are reflected in the individual ozone profiles measured at the three stations on 9 November 2005. As shown in Figure 10, the sonde at (79°N, 12°E) has the lowest ozone mixing ratio (~2.5 ppmv) at 10 hPa, when compared with the other two sondes (>4 ppmv). The analyses capture this low ozone vertical region, with the assimilation run in better agreement, as the control run underestimates the mixing ratio around 20 hPa by about 0.4 ppmv. The profile observed at (52°N, 14°E) shows a typical middle-latitude stratospheric ozone value between 100 and 30 hPa, followed by a transition at higher altitudes to the low ozone typical at the edge of the polar vortex. This transition is well captured by the assimilation run, but is missed entirely in the control run, which leads to an overestimation of ozone at 10 hPa by nearly 1 ppmv. Finally, the profiles at (80°N, 86°W) show high ozone values at levels above 10 hPa, due to the intrusion of the ozone-rich air drawn from low latitudes. Consistent with the overestimation at the low latitudes, the control run is significantly larger than the sonde observation around 10 hPa, which, in contrast, is very well matched by the assimilation run. These results show that after assimilating MLS data, the analyses capture well the horizontal ozone variations associated with the complicated evolution of the polar vortex over the northern hemisphere.

[42] There are small-scale vertical structures shown in the sonde profiles: for example, the double peaks around 90 hPa in the ozone sonde profile at (79°N, 12°E). In general, many of the observed vertical structures are related to the fact that air at different altitudes over one observation site may originate from different horizontal locations [see, e.g., *Tomikawa et al.*, 2002]. However, these small-scale structures usually could not be captured by the current data assimilation systems, owing to the limited vertical resolution of the model and the assimilated observations. Many techniques, such as the reverse trajectory (RT) simulations [see, e.g., *Manney et al.*, 2000], have been developed to reconstruct the vertical structures in the observed ozone profiles, because the resulting high-resolution profiles are useful in the interpretation of the observations, and moreover, their accuracies also reflect the quality of the initial ozone distributions used in these reconstructions.

[43] In the present paper, the sondes observations at (79°N, 12°E) and (52°N, 14°E) were reconstructed by using the reverse trajectory simulations to examine quality of the ozone distributions in the assimilation and control runs. No reconstruction was performed for the sonde at (80°N, 86°W), because its profile was considered too smooth for the reconstruction technique to show anything interesting. In these reconstructions, the vertical range between 350 and 10 hPa over each sonde site under consideration is divided into 150 pressure levels spaced by about 150 m. At each of these 150 pressure levels, 121 parcels are initialized at 1200 UT, 9 November 2005, evenly spaced at a $1^\circ \times 1^\circ$ horizontal grid around the sonde location. They are then propagated backward to 1200 UT, 4 November 2005 by using the 3-dimensional trajectory model of FLEXTRA 3.3 [*Stohl et al.*, 1995], driven by the wind analyses from the assimilation run. Under the passive tracer assumption of no chemical production or loss, the ozone values at that pressure are calculated by averaging over the air parcels whose ozone mixing ratios are determined at the end points of their individual trajectories (i.e, at 1200 UT, 4 November 2005). The end-point values are computed by vertical and

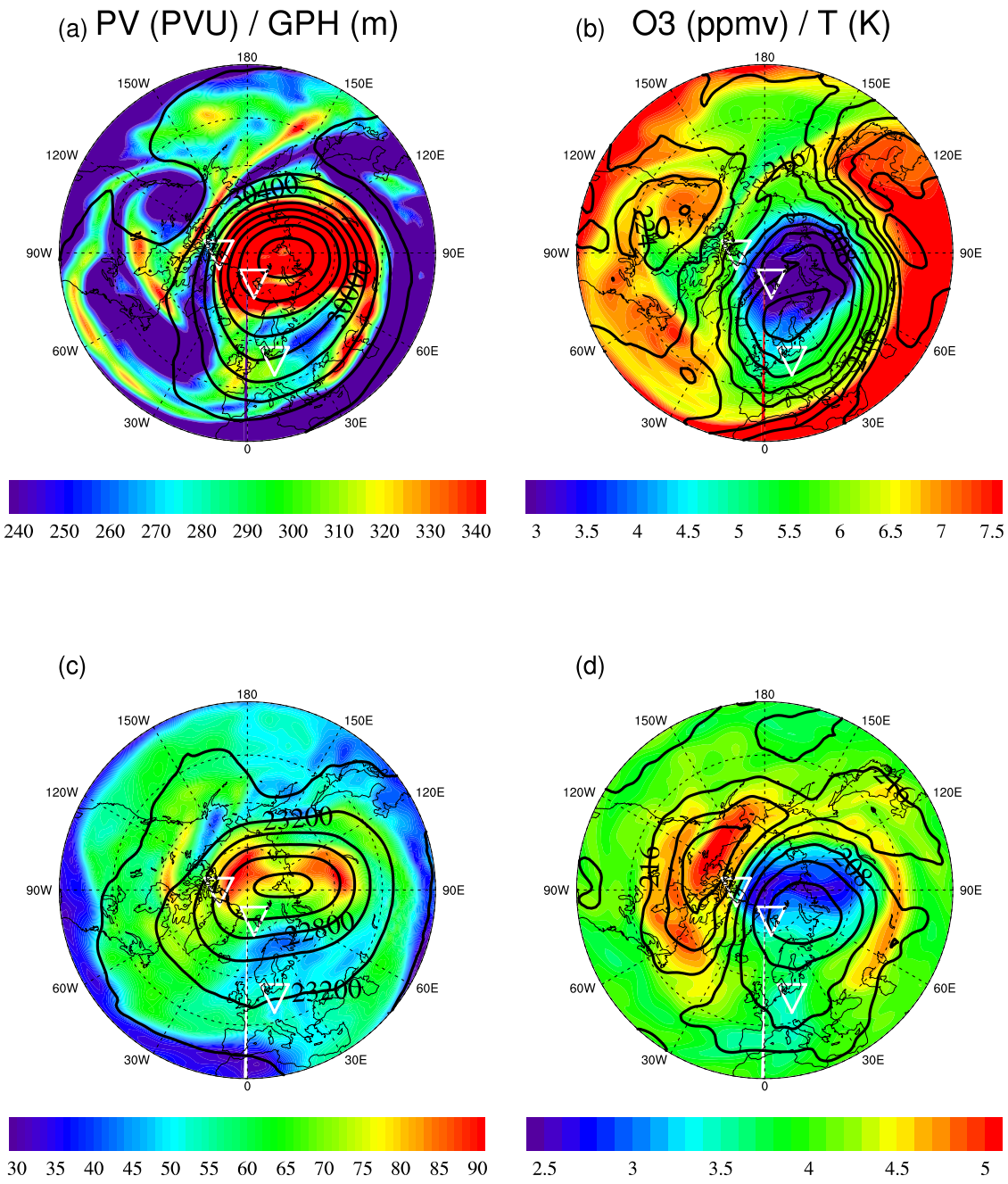

Figure 9. (a) Map of the potential vorticity (PV) in the assimilation run (in PV unit, i.e., 10^{-6} km^2 kg^{-1}) at 10 hPa over the Arctic at 1200 UT, 9 November 2005, overlaid by the contours for the geopotential height with contour interval of 400 m. The triangles denote the locations of three sondes made in the same day: (80°N, 86°W), (79°N, 12°E), and (52°N, 14°E). (b) Map of the ozone analyses in the assimilation run (in ppmv) at 10 hPa over the Arctic at 1200 UT, 9 November 2005, overlaid by the contours for the temperature with contour interval of 4 K. (c and d) The same as Figures 9a and 9b, respectively, but for 32 hPa.

horizontal interpolation of the corresponding ozone analyses from the assimilation run or the control run. Note that the differences in the wind fields between the control and assimilation runs are very small, and hence, using the wind fields from the control run instead of the simulation run in the reverse trajectory simulations would not affect the discussions presented here.

[44] Figures 11a and 11b compare the reconstructed high-resolution profiles with the sondes (the solid lines) at (79°N, 12°E), and (52°N, 14°E), respectively. Note that reconstructed profiles well reproduce the maxima/minima pair between 80 and 100 hPa at (79°N, 12°E), as well as the sharp spike around 70 hPa at (52°N, 14°E). Also, the reconstruction based on the assimilation run matches the observations between 10 and 100 hPa better, indicating an overall improved ozone analysis in the northern hemisphere generally, since the end points of the simulated air parcels spread over a large area. The reverse trajectory simulations

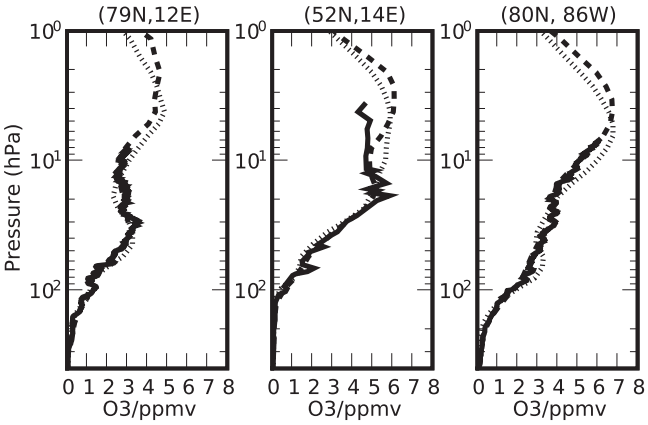

Figure 10. Ozone profiles on 9 November 2005 from the control (dotted lines) and assimilation (dashed lines) run are compared with sondes (solid lines) at the locations shown as triangles in Figure 9.

fail, however, to capture those structures appearing below the 100 hPa level, owing to the relatively poor quality of the ozone analyses in that pressure range.

3.2.3. Low Latitudes: 30°S–30°N

[45] Previous studies [see, e.g., *Dethof and Hólm*, 2004; *Wargan et al.*, 2005; *Geer et al.*, 2006] have revealed that the excessive transport due to the noise in the analyzed wind fields can lead to the underestimation of the ozone peak in the tropical lower stratosphere when no effective observational constraint is available. In our experiment, assimilation of MLS ozone increases the ozone partial pressure by up to 2 mPa in the tropical lower stratosphere, resulting in a better agreement with the ground-based microwave radiometers (Figures 12c and 12d), while showing a slight overestimation in the comparisons with ozone sonde (Figures 12a and 12b). In contrast, at the altitudes below the 215 hPa level, inclusion of MLS data changes the overestimation of the tropical tropospheric ozone by the control run (by up to 20%) to significant underestimation (Figures 12a and 12b), owing to the systematic differences between MLS and operational observations (Figures 2b and 2c).

[46] MLS data also help to reduce the overestimation of the ozone between 5 and 10 hPa, which improves the agreement with the ground-based microwave radiometers (Figures 12c and 12d). However, impacts in the upper stratosphere between 1 and 5 hPa are again too small, and unable to correct the negative biases in the model.

[47] Figure 12 also shows a substantial reduction in the standard deviation between 100 and 10 hPa, indicating the successful filtering of the random errors in the ozone fields which are introduced mainly by the noisy wind analyses in the tropical lower stratosphere. This benefit is highlighted in Figure 13a depicting the anomalies (i.e., the departures from the mean values for the experiment period) detected in ozone and temperature analyses at 20 hPa. As pointed out by *Salby et al.* [1990], when chemical processes can be ignored (for example in the lower tropical stratosphere), large-scale ozone perturbations are mainly induced by vertical air displacements, and hence are in phase with temperature variations. Clear positive correlations between temperature and ozone oscillations have been found in MLS observations [*Feng et al.*, 2007]. Similarly, as indicated by Figure 13a, the perturbations detected in the ozone analyses (the dashed line) are well correlated with those in temper-

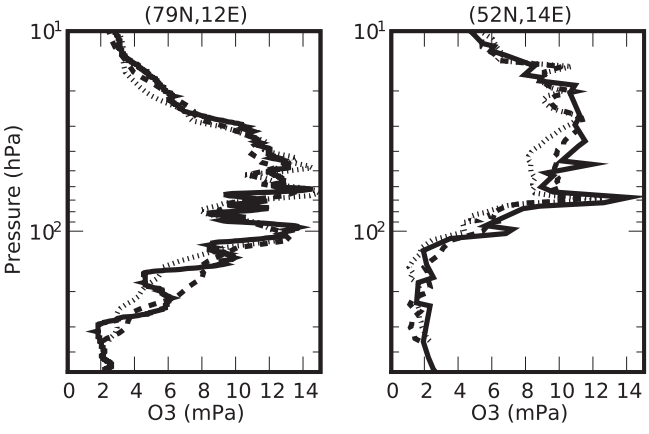

Figure 11. The sondes (solid lines) at (79°N, 12°E), (52°N, 14°E) are compared with the high-resolution ozone profiles constructed from the 5-day reverse trajectory simulations using ozone analyses from the control (dotted lines) and assimilation (dashed lines) run, respectively.

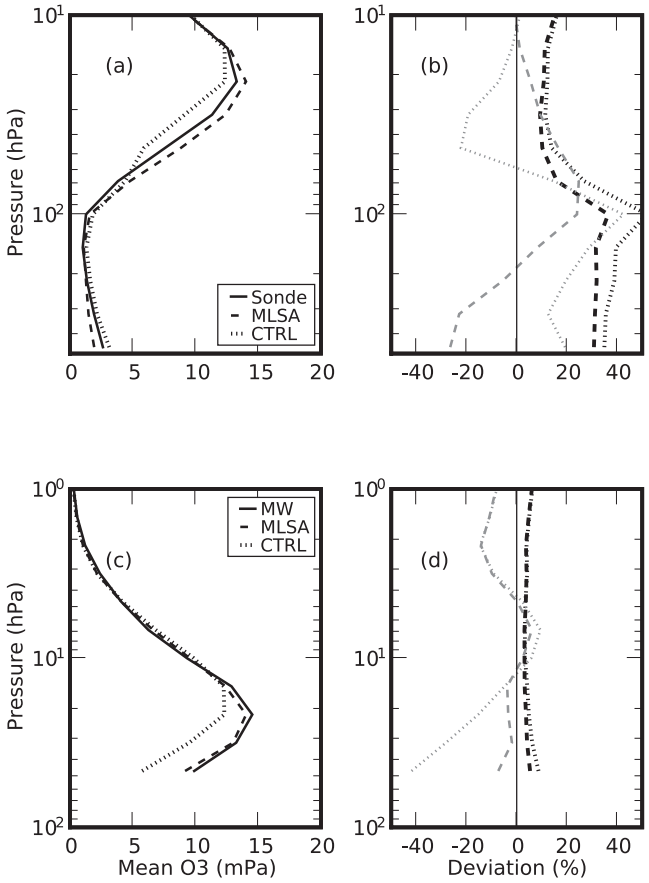

Figure 12. (a and b) The same as Figures 7a and 7b, respectively, but for the comparisons with ozone sondes at 30°S–30°N. (c and d) The same as Figures 12a and 12b but for the comparisons with ground-based microwave radiometers at Mauna Loa (19.5°N, 155.6°W).

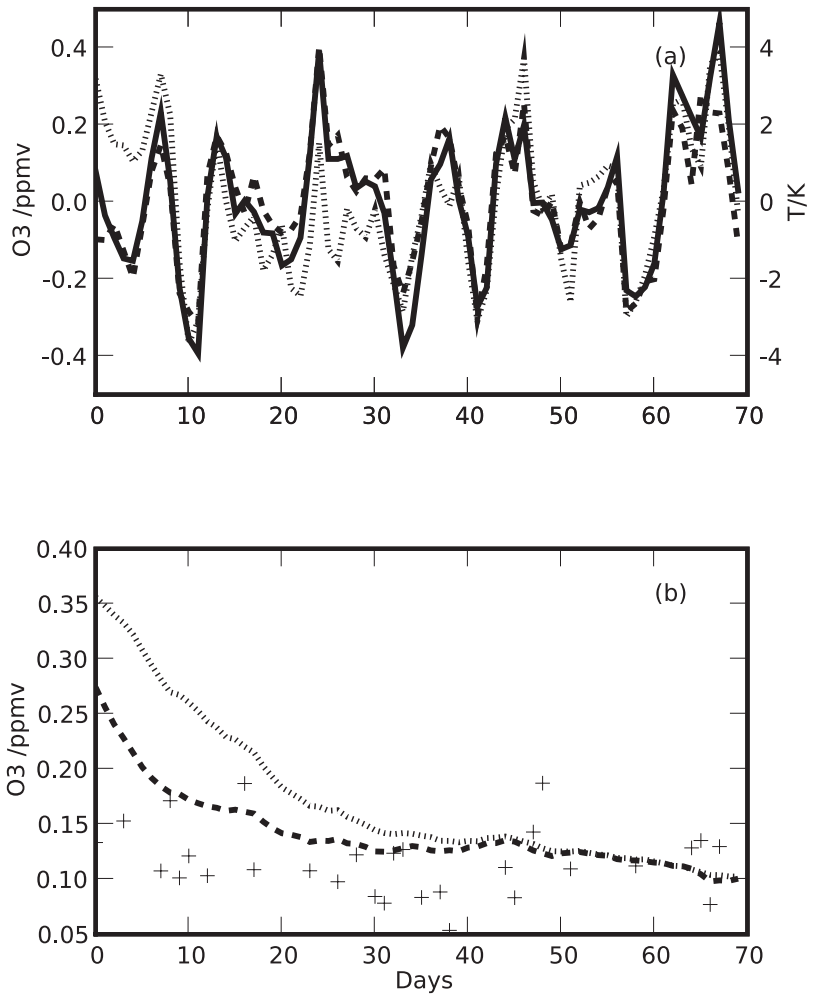

Figure 13. (a) The dotted and dashed lines are the anomalies in ozone analyses at 20 hPa from the assimilation and the control run, respectively, while the solid line (using the right *y* axis) depicts the anomalies detected in the temperature analyses of the assimilation run. The results have been averaged over a region of 5°S–5°N and 10°W–10°E, and the time is given as the days since 15 August 2005. (b) The mean ozone analyses for the control (dotted line) and assimilation (dashed line) run at the 100 hPa level between 10°S and 10°N are given as a function of the days since 15 August 2005, with the daily averaged ozone sonde observations between 10°S and 10°N presented as crosses.

ature (the solid line), once MLS ozone profiles are assimilated. In contrast, while the temperature analyses from the control run are very close to those from the assimilation run (and hence, are not shown), its ozone analyses (the dotted line) exhibit an obviously poorer correlation with the analyzed temperature fields. For example, during days 10 to 39, ozone oscillations in the control run are obviously out of phase and have some extra peaks, like the one around day 19, with no temperature counterpart.

[48] At the tropical tropopause and the lowermost stratosphere around 100 hPa, inclusion of MLS data reduces the standard deviation from over 50% to about 35% (Figure 12b). Such reduction reflects the good quality of MLS observations around the tropical tropopause, and is quite impressive, considering the absence of obvious impacts at such low altitudes from assimilation of MIPAS ozone profiles [*Wargan et al.*, 2005]. On the other hand, the ozone analyses after assimilating MLS data still have a large percentage of uncertainty (around 35% at 100 hPa), which is related to large variations in ozone mixing ratios around 100 hPa, due to variations of the tropical tropopause. In addition, the large standard deviations are also believed to be partially caused by a slow correction of the ozone overestimation introduced at the beginning of the experiments (Figure 13b). In fact, the statistics over second half of the experiment period shows less deviations from ozone sonde for both the assimilation and control runs.

3.2.4. Southern High Latitudes: (60°S–90°S)

[49] Comparison of the ozone analyses with ozone sonde and POAM III observations at the southern high latitudes is presented in Figure 14, where the problems with the control run are highlighted by a transition from the large underestimation around 20 hPa to the large overestimation around 5 hPa (Figures 14c and 14d). In addition, the corresponding standard deviation of the control run is generally higher than 20% between 100 and 10 hPa (Figure 14b), compared to around 10–20% for the assimilation run.

[50] Figure 15 presents the equivalent latitude-time cross section of the ozone analyses at the potential temperature level of 700 K (about 21 hPa) in the assimilation and control

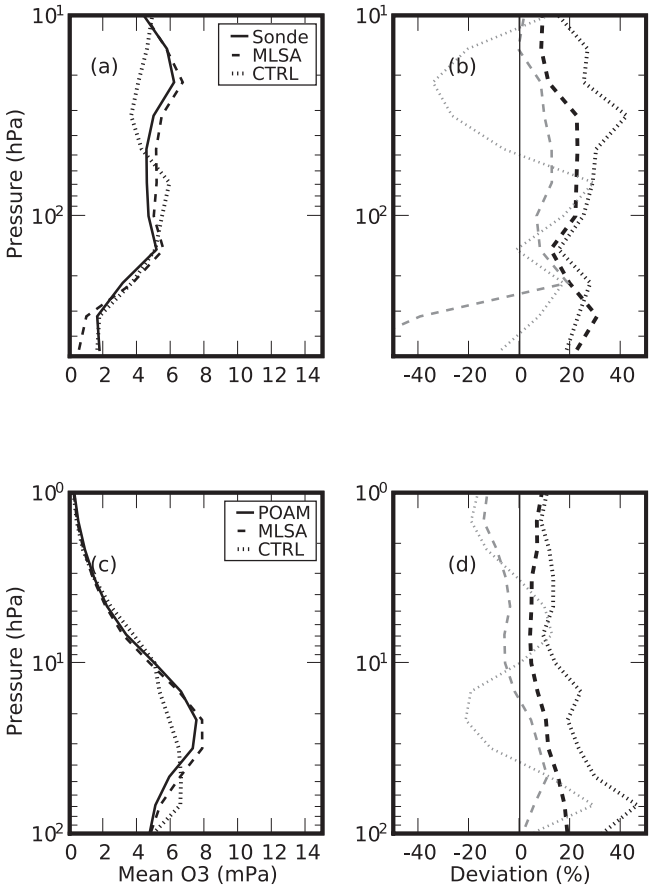

Figure 14. The same as Figure 12, but for the comparisons with (a, b) ozone sonde and (c, d) POAM III at the southern high latitudes.

run. Here, the control run (Figure 15b) shows that during days 0 to 20, the polar vortex, bounded by the dark line, experiences a rapid and significant ozone loss (by up to 2 ppmv), before going through a gradual recovery from day 25. Such an evolution is unrealistic and is believed to be associated with the change in availability of SBUV/2 observations following the arrival of sunlight at southern high latitudes, while contributing to the large errors around 20 hPa (Figure 14). With MLS data assimilated, the impacts from the changing availability of SBUV/2 are suppressed (see Figure 15a), leading to better agreements with independent observations.

[51] It is noted that the assimilation run shows more ozone between 100 and 10 hPa than that observed by ozone sondes. Examination of the individual profiles on 31 August and 1 October (Figure 16) reveals that the assimilation run captures well the scale and vertical location of the observed ozone hole after the heterogeneous depletion of ozone during the southern spring, but there is still a small amount of ozone left in the analyzed profiles, instead of the nearly complete depletion indicated by the sonde profiles.

4. Conclusion

[52] This paper studies the impacts from adding MLS ozone data to the ECMWF 4D-var data assimilation system of version CY30R1, which is used operationally to assimilate the partial ozone column from SBUV/2 and the total ozone column from SCIAMACHY. The early validation of MLS data by *Froidevaux et al.* [2006] shows that MLS profiles are of good quality between 215 and 0.46 hPa, evidenced by the good agreement with independent observations thorough most of the stratosphere. Because of its high vertical resolution (typically 2.7 km in the stratosphere), MLS provides valuable extra constraints on the vertical structure of ozone in the middle and lower stratosphere, which could not be observed by the operational instruments with coarse vertical resolution. In addition, MLS has about 3500 profiles daily covering 82°S to 82°N, while SBUV/2 has only ~1200 daytime observations, with no coverage of the polar night. Consequently, our experiment for the northern autumn of 2005 shows that assimilation of MLS ozone profiles substantially improves the agreement of the ozone analyses with independent observations in most of the stratosphere.

[53] Between 10 and 100 hPa, MLS ozone data induce significant improvements in several meteorologically important areas. For example, in the tropical regions, MLS data help to increase the lower stratospheric ozone peak values, that are underestimated by the control run with only operational observations assimilated. There is also an obvious decrease in the standard deviation between the analyses and ozone sonde observations, indicating the suppression of the random errors associated with the noisy tropical air transport. This benefit is also demonstrated by the better correlation between the temperature and ozone anomalies in

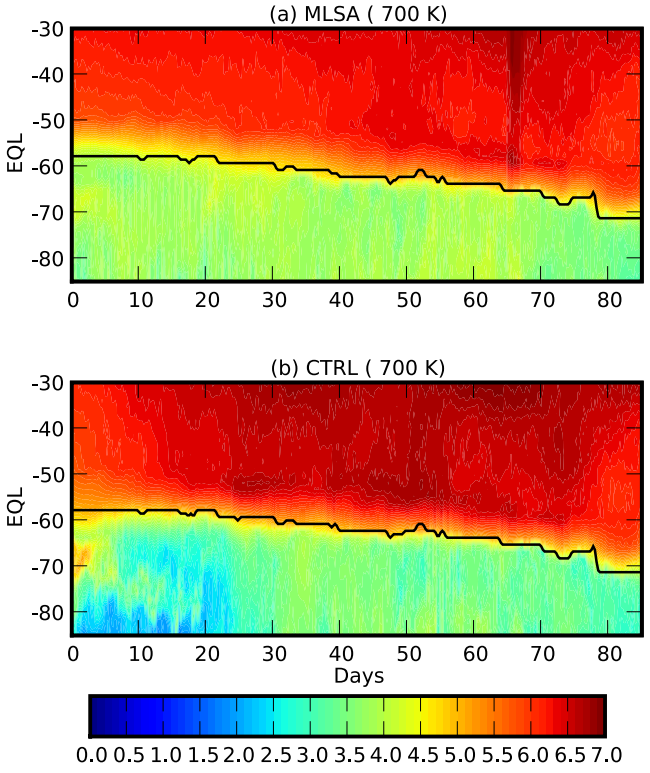

Figure 15. The equivalent latitude (EQL)-time cross section of ozone analyses (in ppmv) at the potential temperature level of 700 K (about 21 hPa). The time is given as the days since 15 August 2005, and the dark line represents the vortex boundary defined as the places with the largest gradient of the potential vortex with respect to EQL.

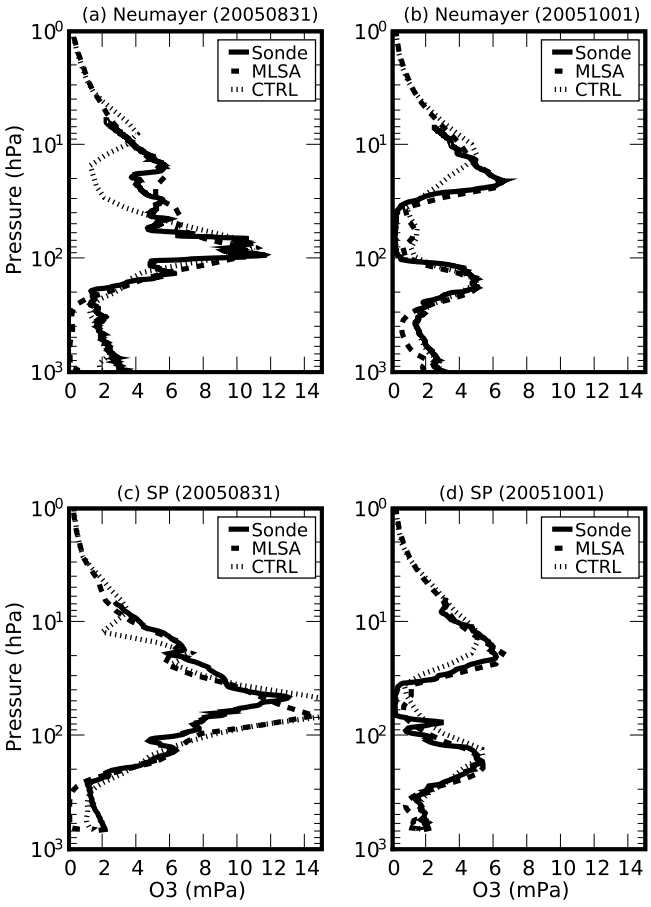

Figure 16. The individual ozone sonde profiles at Neumayer and the southern pole on (left) 31 August and (right) 1 October are compared with collocated analyses.

the resulting analyses. In addition, MLS observations significantly improve the agreement of ozone analyses with POAM III observations at the southern high latitudes, nearly halving the standard deviation between 100 and 10 hPa. Moreover, the continuity of MLS observations into the polar night also ensures a consistent description of the chemical ozone depletion at the southern high latitudes, without obvious artificial changes introduced by variation in the availability of SBUV data at different time periods. A better description of the ozone spatial variations during the polar vortex development is also achieved by the overall improvement in the ozone distribution in the northern hemisphere, when MLS data are assimilated.

[54] Above 10 hPa, the more dense and detailed MLS observations allow less time for model errors to develop significantly, helping correct the model underestimation between 1 and 5 hPa, which is thought to be related to the systematic temperature difference in the upper stratosphere between the ECMWF model of the present experiment and the reference temperature used in parameterization of ozone chemistry.

[55] MLS observations reach down to the 215 hPa level, resulting in significant reduction of the standard deviation at the 100–200 hPa layer. However, inconsistencies among the assimilated ozone observations can cause obvious underestimation of the tropospheric ozone.

[56] In summary, when MLS observations are assimilated, the agreement of the ozone analyses with independent observations between 10 and 100 hPa are within 5–20% at most latitudes except for the tropical regions, compared to 5–30% for the control run. However, the model deficiencies, especially the large biases in the model, prevent further improvement of ozone analyses in the uppermost stratosphere. We will explore the best way to implement a chemistry model into the ECMWF system [*McCormack et al.*, 2006; *Geer et al.*, 2007]. In addition, the biases between MLS and the operational observations have degraded the ozone analyses below 215 hPa. Recently, *Ziemke et al.* [2006] and *Yang et al.* [2007] used MLS ozone data to determine the tropospheric ozone columns together with the total ozone columns from the Aura Ozone Monitoring Instrument (OMI). Their results encourage us in the future to further explore the way to improve the tropospheric ozone analyses from the combined assimilation of the more accurate version 2.2 MLS data and the operational ozone observations through careful bias correction and observation selection such as excluding SBUV/2 data at certain layers.

[57] The impacts of assimilation of MLS ozone profiles on meteorological fields are also of great interest. Recently, *Mathison et al.* [2007] have reported that their preliminary results showed improvements on meteorological analyses and forecasts of their 3D-var system when more realistic ozone fields were used in the radiation calculation, in place of the ozone climatology. However, since the present experiment used ozone climatology in the radiation calculation, assimilation of MLS ozone profiles only induced small impacts in the temperature and wind analyses as well as forecasts. Because of the complicated nature of the modern 4d-var data assimilation systems, thorough understanding of these impacts also requires further investigation. In the meantime, we plan to study the possible benefits from more accurate radiation calculations based on more realistic ozone, and in particular, water vapor distributions generated from assimilation of MLS observations.

[58] **Acknowledgments.** The discussions with A. Dethof and A. Geer in ECMWF were very helpful to our study. We are grateful for the useful comments from I. MacKenzie and P. Palmer in University of Edinburgh, UK. The authors also wish to thank K. Hocke and N. Kämpfer of the University of Bern, Switzerland, and I. McDade and C. Haley of the University of York, Canada, for their kindness in providing us with their ozone observations. The authors also thank the referees for their suggestions in helping to improve this paper. This study is funded by the UK Natural Environment Research Council through the Data Assimilation Research Centre. Work at the Jet Propulsion Laboratory, California Institute of Technology, was carried out under a contract with the National Aeronautics and Space Administration.

References

Bhartia, P. K., R. D. McPeters, C. L. Mateer, L. E. Flynn, and C. Wellemeyer (1996), Algorithm for the estimation of vertical ozone profiles from the backscattered ultraviolet technique, *J. Geophys. Res.*, *101*(D13), 18,793–18,806.

Cariolle, D., and M. Déqué (1986), Southern Hemisphere medium-scale waves and total ozone disturbances in a spectral general circulation model, *J. Geophys. Res.*, *91*(D10), 10,825–10,846.

Cariolle, D., and H. Teyssédre (2007), A revised linear ozone photochemistry parameterization for use in transport and general circulation models: Multi-annual simulations, *Atmos. Chem. Phys.*, *7*, 2183–2196.

Dethof, A. (2003), Assimilation of ozone retrievals from the MIPAS instrument on board ENVISAT, *Tech. Memo. 428*, Eur. Cent. for Medium-range Weather Forecasting, Reading, U. K.

Dethof, A., and E. V. Hólm (2004), Ozone assimilation in the ERA-40 reanalysis project, *Q. J. R. Meteorol. Soc.*, *130*, 2851–2872.

Errera, Q., and D. Fonteyn (2001), Four-dimensional variational chemical assimilation of CRISTA stratospheric measurements, *J. Geophys. Res.*, *106*(D11), 12,253–12,265.

Eskes, H. J., P. F. J. Van Velthoven, P. J. M. Valks, and H. M. Kelder (2003), Assimilation of GOME total ozone satellite observations into a three dimensional tracer transport model, *Q. J. R. Meteorol. Soc.*, *129*, 1663–1681.

Eskes, H. J., R. J. van der A, E. J. Brinksma, J. P. Veefind, J. F. de Haan, and P. J. M. Valks (2005), Retrieval and validation of ozone columns derived from measurements of SCIAMACHY on Envisat, *Atmos. Chem. Phys. Discuss.*, *5*, 4429–4475.

Feng, L., R. S. Harwood, R. Brugge, A. O'Neill, L. Froidevaux, M. Schwartz, and J. W. Waters (2007), Equatorial Kelvin waves as revealed by EOS Microwave Limb Sounder observations and European Centre for Medium-range Weather Forecasts analyses: Evidence for slow Kelvin waves of zonal wave number 3, *J. Geophys. Res.*, *112*, D16106, doi:10.1029/2006JD008329.

Fioletov, V. E., D. W. Tarasick, and I. Petropavlovskikh (2006), Estimating ozone variability and instrument uncertainties from SBUV (/2), ozonesonde, Umkehr, and SAGE II measurements: Short-term variations, *J. Geophys. Res.*, *111*, D02305, doi:10.1029/2005JD006340.

Froidevaux, L., et al. (2006), Early validation analyses of atmospheric profiles from EOS MLS on the Aura satellite, *IEEE Trans. Geosci. Remote Sens.*, *44*, 1106–1121.

Froidevaux, L., et al. (2008), Validation of the Aura Microwave Limb Sounder stratospheric ozone measurements, *J. Geophys. Res.*, doi:10.1029/2007JD008771, in press.

Geer, A. J., C. Peuby, R. N. Bannister, R. Brugge, D. R. Jackson, W. A. Lahoz, S. Migliorini, A. O'Neill, and R. Swinbank (2006), Assimilation of stratospheric ozone from MIPAS into a global general-circulation model: The September 2002 vortex split, *Q. J. R. Meteorol. Soc.*, *132*, 231–257.

Geer, A. J., W. A. Lahoz, D. R. Jackson, D. Cariolle, and J. P. McCormack (2007), Evaluation of linear ozone photochemistry parameterizations in a stratosphere-troposphere data assimilation system, *Atmos. Chem. Phys.*, *7*, 939–959.

Hólm, E. V., A. Untch, A. Simmons, R. Saunders, F. Bouttier, and E. Andersson (1999), Multivariate ozone assimilation in four dimensional data assimilation, paper presented at SODA Workshop on Chemical Data Assimilation, R. Neth. Meteorol. Inst., De Bilt, Netherlands.

Hólm, E. V., A. Untch, A. Simmons, R. Saunders, F. Bouttier, and E. Andersson (2000), Multivariate ozone assimilation, paper presented at Third international Symposium on Assimilation of Observations in Meteorology and Oceanography, World Meteorol. Org., Geneva.

Jackson, D. R. (2007), Assimilation of EOS MLS ozone observations in the Met Office data-assimilation system, *Q. J. R. Meteorol. Soc.*, *133*, 1771–1788.

Jackson, D. R., and R. Saunders (2002), Ozone data assimilation: Preliminary system, *Forecasting Res. Tech. Rep. 394*, Met Office, Exeter, UK.

Komhyr, W. D., R. A. Barnes, G. B. Brothers, J. A. Lathrop, and D. P. Opperman (1995), Electrochemical concentration cell ozonesonde performance evaluation during STOIC 1989, *J. Geophys. Res.*, *100*(D5), 9231–9244.

Levelt, P. F., B. V. Khattatov, J. C. Gille, G. P. Brasseur, X. X. Tie, and J. W. Waters (1998), Assimilation of MLS ozone measurements in the global three-dimensional chemistry transport model ROSE, *Geophys. Res. Lett.*, *25*, 4493–4496.

Manney, G. L., H. A. Michelsen, F. W. Irion, G. C. Toon, M. R. Gunson, and A. E. Roche (2000), Lamination and polar vortex development in fall from ATMOS long-lived trace gases observed during November 1994, *J. Geophys. Res.*, *105*(D23), 29,023–29,038.

Mathison, C., D. R. Jackson, and M. Keil (2007), Methods of improving the representation of ozone in the UK Met Office model, *Forecasting Res. Tech. Rep. 502*, Met Office, Exeter, U. K.

McCormack, J. P., S. D. Eckermann, D. E. Siskind, and T. J. McGee (2006), CHEM2D-OPP: A new linearized gas-phase ozone photochemistry parameterization for high altitude NWP and climate models, *Atmos. Chem. Phys.*, *6*, 4943–4972.

Morcrette, J. J. (2003), Ozone-radiation interactions in the ECMWF forecast system, *Tech. Memo. 375*, Eur. Cent. for Medium-range Weather Forecasting, Reading, U. K.

Nazaryan, H., and M. P. McCormick (2005), Comparisons of Stratospheric Aerosol and Gas Experiment (SAGE II) and Solar Backscatter Ultraviolet Instrument (SBUV/2) ozone profiles and trend estimates, *J. Geophys. Res.*, *110*, D17302, doi:10.1029/2004JD005483.

Paul, J., J. Fortuin, and H. Kelder (1998), An ozone climatology based on ozonesonde and satellite measurements, *J. Geophys. Res.*, *103*(D24), 31,709–31,734.

Peuch, A., J. N. Thépaut, and J. Pailleux (2000), Dynamical impact of total-ozone observations in a four-dimensional variational assimilation, *Q. J. R. Meteorol. Soc.*, *126*, 1641–1659.

Randall, C. E., et al. (2003), Validation of POAM III ozone:comparison with ozonesonde and satellite data, *J. Geophys. Res.*, *108*(D12), 4367, doi:10.1029/2002JD002944.

Randall, C. E., et al. (2005), Reconstruction and simulation of stratospheric ozone distribution during the 2002 austral winter, *J. Atmos. Sci.*, *62*(3), 748–764, doi:10.1175/JAS-3336.1.

Riishøjgaard, L. P. (1996), On four-dimensional variational assimilation of ozone data in weather-prediction models, *Q. J. R. Meteorol. Soc.*, *122*, 1545–1571.

Salby, M. L., P. Callaghan, S. Solomon, and R. Garcia (1990), Chemical fluctuations associated with vertically propagating equatorial Kelvin waves, *J. Geophys. Res.*, *95*(D12), 20,491–20,505.

Schoeberl, M. R., A. R. Douglass, Z. Zhu, and S. Pawson (2003), A comparison of the lower stratospheric age spectra derived from a general circulation model and two data assimilation systems, *J. Geophys. Res.*, *108*(D3), 4113, doi:10.1029/2002JD002652.

Stajner, I., and K. Wargan (2004), Antarctic stratospheric ozone from the assimilation of occultation data, *Geophys. Res. Lett.*, *31*, L18108, doi:10.1029/2004GL020846.

Stajner, I., L. P. Riishøjgaard, and R. B. Rood (2001), The GEOS ozone data assimilation system: Specification of error statistics, *Q. J. R. Meteorol. Soc.*, *127*, 1069–1094.

Stajner, I., K. Wargan, L.-P. Chang, H. Hayashi, S. Pawson, and H. Nakajima (2006), Assimilation of ozone profiles from the Improved Limb Atmospheric Spectrometer-II: Study of Antarctic ozone, *J. Geophys. Res.*, *111*, D11S14, doi:10.1029/2005JD006448.

Stohl, A., G. Wotawa, P. Seibert, and H. Kromp-Kolb (1995), Interpolation errors in wind fields as a function of spatial and temporal resolution and their impact on different types of kinematic trajectories, *J. Appl. Meteorol.*, *34*, 2149–2165.

Struthers, H., R. Brugge, W. A. Lahoz, A. O'Neill, and R. Swinbank (2002), Assimilation of ozone profiles and total column measurements into a global general circulation model, *J. Geophys. Res.*, *107*(D20), 4438, doi:10.1029/2001JD000957.

Terao, Y., and J. A. Logan (2007), Consistency of time series and trends of stratospheric ozone as seen by ozonesonde, SAGE II, HALOE, and SBUV (/2), *J. Geophys. Res.*, *112*, D06310, doi:10.1029/2006JD007667.

Thomason, L. W., and G. Taha (2003), SAGE III aerosol extinction measurements: Initial results, *Geophys. Res. Lett.*, *30*(12), 1631, doi:10.1029/2003GL017317.

Thompson, A. M., et al. (2003), Southern Hemisphere Additional Ozonesondes (SHADOZ) 1998–2000 tropical ozone climatology: 1. Comparison with Total Ozone Mapping Spectrometer (TOMS) and ground-based measurements, *J. Geophys. Res.*, *108*(D2), 8238, doi:10.1029/2001JD000967.

Tomikawa, Y., K. Sato, K. Kita, M. Fujiwara, M. Yamamori, and T. Sano (2002), Formation of an ozone lamina due to differential advection revealed by intensive observations, *J. Geophys. Res.*, *107*(D10), 4092, doi:10.1029/2001JD000386.

Wargan, K., I. Stajner, S. Pawson, R. B. Rood, and W. W. Tan (2005), Monitoring and assimilating of ozone data from the Michelson Interferometer for Passive Atmospheric Sounding, *Q. J. R. Meteorol. Soc.*, *131*, 2713–2734.

Waters, J., et al. (2006), The Earth Observation System Microwave Limb Sounder (EOS MLS) on the Aura Satellite, *IEEE Trans. Geosci. Remote Sens.*, *44*, 1075–1092.

Yang, Q., D. M. Cunnold, H.-J. Wang, L. Froidevaux, H. Claude, J. Merrill, M. Newchurch, and S. J. Oltmans (2007), Midlatitude tropospheric ozone columns derived from the Aura Ozone Monitoring Instrument and Microwave Limb Sounder measurements, *J. Geophys. Res.*, *112*, D20305, doi:10.1029/2007JD008528.

Ziemke, J. R., S. Chandra, B. N. Duncan, L. Froidevaux, P. K. Bhartia, P. F. Levelt, and J. W. Waters (2006), Tropospheric ozone determined from Aura OMI and MLS: Evaluation of measurements and comparison with the Global Modeling Initiative's Chemical Transport Model, *J. Geophys. Res.*, *111*, D19303, doi:10.1029/2006JD007089.

R. Brugge and A. O'Neill, Data Assimilation Research Centre, University of Reading, Reading RG6 6BB, UK.

L. Feng, M. J. Filipiak, and R. S. Harwood, Institute of Atmospheric and Environmental Science, University of Edinburgh, Crew Building, King's Buildings, Edinburgh EH9 3JN, UK. (liang@met.ed.ac.uk)

L. Froidevaux and N. Livesey, Jet Propulsion Laboratory, California Institute of Technology, 4800 Oak Grove Drive, Pasadena, CA 91109, USA.

E. V. Hólm, European Centre for Medium-range Weather Forecasts, Reading RG2 9AX, UK.